J Mater Sci (2007) 42:4044–4050
DOI 10.1007/s10853-006-0190-9

Transient liquid phase bonding of steel using an Fe–B interlayer

Nicolas Di Luozzo · Marcelo Fontana · Bibiana Arcondo

Received: 29 July 2005 / Accepted: 10 April 2006 / Published online: 31 January 2007

Abstract Transient liquid phase bonding processes have been performed to join two carbon steel tubes using $Fe_{96.2}B_{3.8}$ wt% amorphous ribbons as interlayers. Welding experiments were performed at the temperature $T \approx 1{,}250$ °C for different durations and under pressures of 2, 3 and 4 MPa. From metallographic inspection it is concluded that the bonding process ends in 7.0 min if a pressure of 4 MPa is applied whereas the process results incomplete if less pressure is applied. A 1D model using a finite element method has been developed for the simulation of a transient liquid phase bonding process. This model was applied to the bonding of steel/Fe–B glassy metals/steel. The computed results allow us to understand the role played by the variables involved in the bonding process.

Introduction

Problems of diffusion controlled moving boundaries occur in a wide range of metallurgical situations, for example in joining processes. In recent years, the transient liquid phase bonding (TLPB) process has been widely studied [1–4] in order to improve the characteristics of the joints by means of composition and microstructure homogenization along the joined pieces. TLPB is commonly used in the repair of aeroengine turbine blades and involves three main steps, namely, liquefaction of the filler material and base metal dissolution in the liquid gap, liquid phase isothermal solidification, and solute homogenization [5–7].

The TLPB process is governed by a system of diffusion differential equations with moving boundary conditions at the liquid–solid interface. Numerical solution methods have been used to solve these equations. The TLPB process, without pressure application, has already been modeled by Zhou et al. [8] using a finite difference procedure, which coincided well with the experimental data. Ohsasa et al. [2] presented a model of dissolution and isothermal solidification during the TLPB process of nickel using Ni–Cr–B filler metal. They combined thermodynamic calculation with Thermo-Calc software package and diffusion analysis by a finite difference method. Illingworth et al. [9] presented an interesting analysis about the different ways to solve the diffusion equations using a finite difference method. They indicated that the main difficulty of the finite difference method in the TLPB process consists of tracking the motion of solid/liquid interfaces.

In our paper, the problem of the mobile interface is solved using the finite element method: The interface is always on a node, therefore, the mesh has to be re-defined at each instant due to the continuous interface movement. The width of the liquid gap, the solidification time and the solute concentration profiles are obtained.

An innovation in TLPB processes is the application of glassy metal ribbons as filling material [10]. The ductility of glass allows the easy compliance of the

N. Di Luozzo · M. Fontana · B. Arcondo (✉)
Laboratorio de Sólidos Amorfos, Departamento de Física, Facultad de Ingeniería, Universidad de Buenos Aires, Paseo Colon 850, Buenos Aires 1063, Argentina
e-mail: barcond@fi.uba.ar

N. Di Luozzo
e-mail: nicolasdiluozzo@yahoo.com.ar

M. Fontana
e-mail: mfontan@fi.uba.ar

metallic ribbon to the surfaces of the pieces while its limited thickness reduces the bonding time. With the aim of improving the contact of the tubes with the glass and of reducing the process time from hours to minutes, the TLPB process has been performed under the application of pressure [11–13]. However, to our knowledge, there is no work either experimental or theoretical connecting applied pressure and reduction of the TLPB duration.

In the present study, the joining of steel tubes was performed by means of TLPB with pressure application and employing glassy metals as filling material. It was modelled with a new numerical method employing finite elements. Our aim is to determine experimentally the time needed to end the process in the steel/Fe–B/steel bonding with pressure application and to compare the experimental results with the numerical simulation.

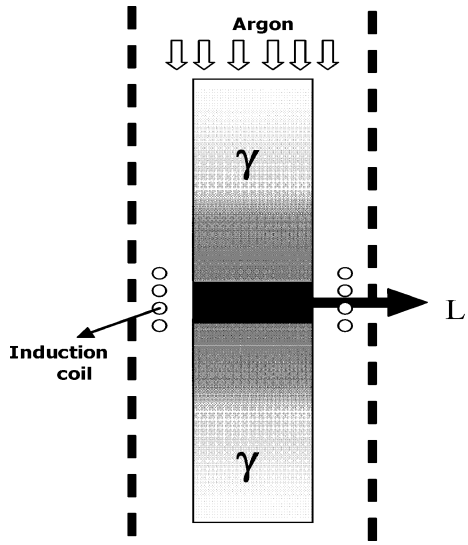

Fig. 1 Schematic welding device. Two bars of metal and an amorphous interlayer L placed in an induction furnace

Experimental procedure and experimental results

Transient liquid phase bonding processes under Ar atmosphere have been performed to join two carbon steel tubes (see composition in Table 1) of 19 mm external diameter and 2.5 mm wall thickness. $Fe_{96.2}B_{3.8}$ wt% amorphous ribbons of thickness $a \approx 20$ μm have been employed as interlayers. The tubes were aligned with the surfaces of both pieces in contact with the amorphous layer. The surfaces were prepared by turning and its average roughness is Ra = 1.6 μm on an evaluation length of 2.5 mm with a cut off length of 2.5 mm. The arrangement was placed into the coil of an induction furnace under Ar atmosphere as is shown in Fig. 1. The temperature was raised at the highest possible rate to T (with $T \approx 1{,}250$ °C) and then held constant for different durations up to 7.0 min. The welding processes were performed under pressures of 2, 3 and 4 MPa and several samples were obtained for each set of parameters.

The outer surface of the joined tubes was mechanically smoothed parallel to the axis of the tubes in order to prepare a 12 mm (width) × 30 mm (length) plane surface where the microstructure of the joint region resulted exposed. The width of the plane surface displays the microstructure at different depths into the tube wall; the external borders correspond to the outer surface of the tubes whereas the central line corresponds to a surface not far (0.36 mm) from the inner surface of the tubes. The plane surface was polished with sand paper of different granulometry and finally micropolished with 0.05 μm gamma alumina. These surfaces were examined using optical microscopy and scanning electron microscopy (Philips XL 30CP).

From metallographic inspection it is concluded that the bonding process ends in 7.0 min if a pressure of 4 MPa is applied whereas the process results incomplete if the applied pressure is less. For shorter times a structural separation between the joined pieces due to the presence of non-isothermally solidified liquid is observed. Micrographs of the joint zone are presented in Fig. 2.

Table 1 Steel tubes composition (wt%)

C	Mn	Si	Ni	Cr	Mo	Cu	B
0.120	0.450	0.180	0.025	0.030	0.010	0.054	0.0001
Sn	V	Al	Nb	Ti	As	S	P
0.004	0.001	0.025	0.001	0.001	0.003	0.0019	0.011

Physical description

Let us assume that two tubes of a solid γ (with composition C_S) are aligned with their surfaces in contact with a thin amorphous layer of thickness a (see L in Fig. 1). The length of the arrangement is d. The amorphous layer composition C_L is not far from an eutectic point (E) whose components are γ and β (Fig. 3). The melting temperature of the amorphous layer (T_L) is lower than the melting temperature of γ (T_S). If the temperature in the joining zone is raised to T at the highest possible rate, being $T_L < T < T_S$, a transient liquid phase forms. As the temperature T is held constant, the following process will take place:

Fig. 2 Scanning electron micrographs (back scattering electron detection) of the union zone for steel/iron-boron/steel bonding at 1,250 °C. The joints were performed under applied pressures of 2 MPa (top) and 4 MPa (bottom). The process time is 7 min

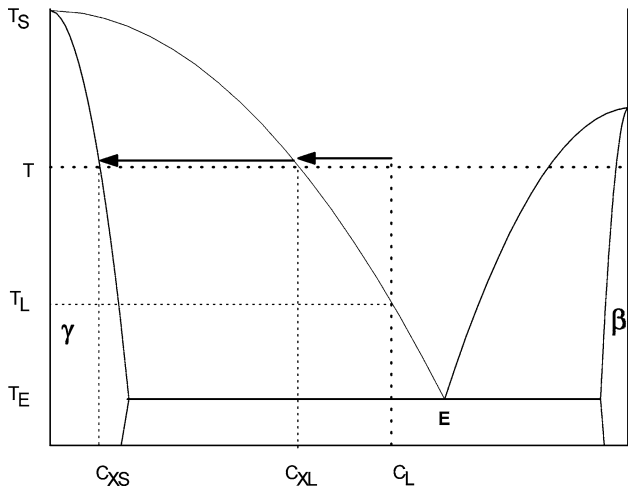

Fig. 3 Phases equilibrium diagram of the α-β system. T is the isothermal welding temperature, C_L the initial composition of the transient liquid gap, C_{XL} the composition of the liquid gap as a solid phase of composition C_{XS} precipitates

- The dissolution of the base material into the liquid gap occurs, thus widening the gap.
- When the concentration in the liquid reaches C_{XL}, the solidification starts and the gap proceeds to close up to its total disappearance (the concentration of the solid in the interface is C_{XS}).
- The completion of the solid state diffusion is performed [7, 14].

The amorphous nature of the layer is not a precondition for the transient liquid phase bonding process. However, amorphous layers present many advantages when compared to the corresponding crystalline materials. Metallic glasses have a very large ductility therefore, in the form of thin layers, amorphous metals are easier to handle than crystals. In addition, amorphous layers improve the contact with the tubes when pressure is applied whereas crystalline layers break. Our assumptions of process models are [8, 15]:

1. The problem is reduced to two components, in our case: Fe and B. Although steel is a multi-component alloy (in our case, the steel is ASTM A 106 Gr A), we assume that the effect of minority components is negligible. We consider that the minority components of steel (C, Mn, etc.) do not influence the B diffusion, do not influence the mass balance and do not generate new phases with the B atom.
2. Local equilibrium exists at the solid–liquid interface. The solid and liquid compositions at the interface (C_{XL} and C_{XS}) are determined by the equilibrium phase diagram.
3. The moveable interface remains planar throughout the entire process. Therefore, only one spatial variable, called x, is necessary to describe diffusion. This assumption is suitable when the solid is a single crystal [16]. If the solid is polycrystalline (as in our case) the situation is more complicated: the diffusion along grain boundaries has to be analyzed [17]. In this case, a total diffusion coefficient is used considering the effect of diffusion in the lattice and, in addition, diffusion in grain boundaries.
4. The temperature of the joint (solid/liquid/solid) is constant and uniform for all x. That is, the temperature distribution is not affected by the latent heat effect.
5. The liquid and solid diffusion coefficients and the molar volume of the phases do not depend on concentration. The molar volume of both phases (solid and liquid) is the same.
6. The interface movement is due only to diffusion.

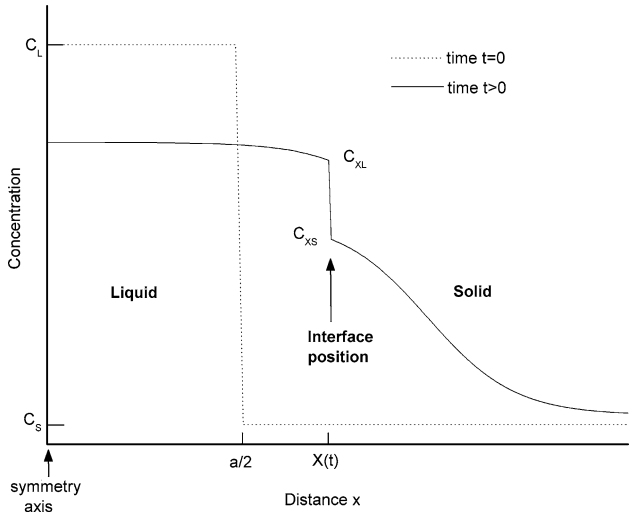

Fig. 4 Dependence with the distance x of the solute concentration $c(x,t)$ for $t = 0$ and $t > 0$. The solid–liquid interface position $X(t)$ is shown. At time t, the liquid phase L is limited to the range $0 < x < X(t)$ as well as the solid phase is at $X(t) < x < d/2$

Figure 4 shows the solid–liquid interface position $X(t)$ and the solute concentration $c(x,t)$ under the assumptions that the liquid phase L is limited to the range $0 < x < X(t)$ and the solid phase is at $X(t) < x < d/2$ (with $X(t) \ll d/2$ for all time t). The liquid gap width is $w(t) = 2X(t)$. Therefore, the equations, which describe the diffusion in a transient liquid phase bonding process, are the Fick laws:

$$\frac{\partial c_L(x,t)}{\partial t} = D_L \frac{\partial^2 c_L(x,t)}{\partial x^2} \quad 0 < x < X(t) \tag{1}$$

$$\frac{\partial c_S(x,t)}{\partial t} = D_S \frac{\partial^2 c_S(x,t)}{\partial x^2} \quad X(t) < x < d/2 \tag{2}$$

with S and L indicating solid and liquid phases, and D the diffusion coefficient.

Equations 1 and 2 have the following boundary conditions:

$$\left.\frac{\partial c_L(x,t)}{\partial x}\right|_{x=0} = 0$$

$$\left.\frac{\partial c_S(x,t)}{\partial x}\right|_{x=d/2} = 0$$

and at the interface:

$$c_L(X(t),t) = C_{XL} \tag{3}$$

$$c_S(X(t),t) = C_{XS} \tag{4}$$

The initial conditions are:

$$c_L(x,0) = C_L \quad 0 < x < a/2 \tag{5}$$

$$c_S(x,0) = C_S \quad a/2 < x < d/2 \tag{6}$$

The interface velocity can be determined using the mass conservation at the moving interface [18]:

$$(C_{XL} - C_{XS})\frac{\partial X(t)}{\partial t} = -D_L \left.\frac{\partial c_L(x,t)}{\partial x}\right|_{x=X(t)} + D_S \left.\frac{\partial c_S(x,t)}{\partial x}\right|_{x=X(t)} \tag{7}$$

Numerical analysis

Diffusion equations. Approximation using finite element method

The finite element method (FEM) [19] has been used for the solution of the Eqs. 1 and 2. The first step is the subdivision of the domain into a set of discrete subdomains. As mentioned above the problem is 1D, therefore we used 1D element with two nodes (1 and 2) on the borders. A general variable c (in our case c is the composition) can be expressed with the node values c_1 and c_2. Therefore, the composition c and the temporal derivative $\partial c/\partial t$ are expressed in the following form:

$$c(r) = h_1(r) \cdot c_1 + h_2(r) \cdot c_2 = \underline{H} \cdot \underline{C}$$

with h_1 and h_2 the local interpolation functions.

$$\frac{\partial c}{\partial t} = \underline{H} \cdot \frac{\partial \underline{C}}{\partial t} = \underline{H} \cdot \dot{\underline{C}}$$

where $\underline{C}$ is the vector of the concentration of the nodes;

$$\underline{C} = \begin{pmatrix} c_1 \\ c_2 \end{pmatrix}, \quad \underline{H} = [h_1 h_2] \text{ and } \dot{\underline{C}} = \begin{pmatrix} \partial c_1/\partial t \\ \partial c_2/\partial t \end{pmatrix}$$

Using the Galerkin method [19]:

$$\int_\Omega \underline{H}^T \cdot \frac{\partial c}{\partial t}\, d\Omega - D \int_\Omega \underline{H}^T \cdot \frac{\partial^2 c}{\partial x^2}\, d\Omega = 0$$

Thus,

$$\int_\Omega \underline{H}^T \cdot \underline{H}\, d\Omega \cdot \dot{\underline{C}} + D \int_\Omega \frac{\partial \underline{H}^T}{\partial x} \cdot \frac{\partial \underline{H}}{\partial x}\, d\Omega \cdot \underline{C} = 0$$

$$\underline{\underline{C}} \cdot \dot{\underline{C}} + \underline{\underline{K}} \cdot \underline{C} = 0 \tag{8}$$

with

$$\underline{\underline{C}} = \sum_e \int_{\Omega_e} \underline{H}^T \cdot \underline{H}\, d\Omega$$

$$\underline{\underline{K}} = \sum_e D \int_{\Omega_e} \frac{\partial \underline{H}^T}{\partial x} \cdot \frac{\partial \underline{H}}{\partial x}\, d\Omega = \sum_e D \int_{\Omega_e} \underline{B}^T \cdot \underline{B}\, d\Omega$$

where Ω_e is the element domain and

$$\underline{B} = \frac{\partial \underline{H}}{\partial x}$$

Application of the α method

$\dot{\underline{C}}$ in Eq. 8 can be determined using the α method [19]. $\underline{C}$ for the time t is noted ${}^t\underline{C}$ and $\dot{\underline{C}}$ for the time $t + \alpha\Delta t$, ${}^{t+\alpha\Delta t}\dot{\underline{C}}$, is written as:

$${}^{t+\alpha\Delta t}\dot{\underline{C}} = ({}^{t+\Delta t}\underline{C} - {}^t\underline{C})/\Delta t$$

where $0 \le \alpha \le 1$. In our case, we used a Cranck–Nicholson scheme [19] with $\alpha = 0.5$.

Replacing in Eq. 8, one obtains:

$$\left[\underline{\underline{C}} + \underline{\underline{K}}\alpha \cdot \Delta t\right] \cdot {}^{t+\Delta t}\underline{C} = \left[\underline{\underline{C}} - \underline{\underline{K}}(1-\alpha) \cdot \Delta t\right] \cdot {}^t\underline{C}$$

Approximation of the interface movement

The liquid phase is limited to the range $0 < x < X(t)$ and the solid phase is at $X(t) < x < d/2$.

Equation 7 can be rewritten as:

$$\frac{\partial X(t)}{\partial t} = f(X(t), t) \tag{9}$$

The solid–liquid interface position $X(t + \Delta t)$ at time $t + \Delta t$ was calculated using an iterative process with the function $f(X(t),t)$ (Eq. 9) and assuming $X(t)$ at a time t. As a first approximation $X(t + \Delta t)$ was determined employing:

$$X^{(0)}(t + \Delta t) = X(t) + \Delta t\, f(X(t), t)$$

and the ith approximation of $X(t + \Delta t)$ is obtained from its $(i–1)$th approximation:

$$X^{(i)}(t + \Delta t) = X(t) + \frac{\Delta t}{2}\left[f(X(t), t) + f(X^{(i-1)}(t + \Delta t), t + \Delta t)\right]$$

with

$$f(X^{(i-1)}(t + \Delta t), t + \Delta t) = \frac{1}{C_{XL} - C_{XS}}\left(-D_L \frac{\partial c_L(x, t + \Delta t)}{\partial x}\bigg|_{x = X^{(i-1)}(t+\Delta t)} + D_S \frac{\partial c_S(x, t + \Delta t)}{\partial x}\bigg|_{x = X^{(i-1)}(t+\Delta t)}\right)$$

This iterative process stops at the step k when:

$$\left|\frac{X^{(k+1)}(t + \Delta t) - X^{(k)}(t + \Delta t)}{X^{(k)}(t + \Delta t)}\right| < 10^{-6}$$

Mesh

With the aim to obtain a characteristic length of the mesh, we defined a length unit l as 1/20 of the amorphous layer initial thickness a, that is $l = a/20$. Therefore, we divided the mesh into four zones, from the transverse symmetry axis up to the boundary approaching "infinity": zone 1 is made of 80 elements with an element length Le of 1 length unit (the interface moves in zone 1); zone 2 is made of 40 elements with an element length of 5 length units; zone 3 is made of 40 elements with an element length of 25 length units and zone 4 is made of 240 elements with an element length of 125 length units.

The mesh around the symmetry axis is very compact in order to obtain a good fit of the interface movement. As the mesh far from the joint is sufficiently large, "infinity" can be modeled. The interface moves in zone 1, and zones 2, 3 and 4 attempt to model "infinity".

In our work the interface is always on a node. Therefore, the mesh has to be re-defined at each instant due to the continuous interface movement. Despite the remeshing, the mesh at time t differs from the original mesh only at one node, the node where the interface lays.

We assume that the interface at the instant t is on the node n and, as the interface moves, at the instant $t + \Delta t$ the interface position is $X(t + \Delta t)$. Thus, in each process, e.g. the dissolution, the mesh should be updated and two situations can be exhibited:

1. If the interface position is between $x_{n-1} + Le$ and $x_{n-1} + 3/2Le$, where x_{n-1} is the position of node n–1, node n is displaced to the new interface position $X(t + \Delta t)$.
2. If the interface position is between $x_{n-1} + 3/2\ Le$ and $x_{n-1} + 2\ Le$, node $n + 1$ is displaced to the new interface position $X(t + \Delta t)$ and node n is moved to its original position in the mesh.

In the solidification the same procedure is employed.

Results

The value of the magnitudes involved in the numerical simulation are the following:

1. Assuming that the base material is pure Fe, $C_S = 0$. The interlayer is the alloy $Fe_{96.2}B_{3.8}$ wt%.
2. The solid and liquid composition at the interface are $C_{XL} = 3.011$ wt% and $C_{XS} = 0.021$ wt% [20].
3. The process temperature is $T = 1{,}250$ °C.
4. Diffusion of B in Fe is purely interstitial diffusion [21] and it is almost independent of pressure [22]. The total diffusion coefficient of B in polycrystalline Fe is $D_S = 194$ μm^2/s [23].
5. As far as we know, the diffusion coefficient of B in liquid Fe, D_L, is not to be found in literature. Nevertheless, as the diffusion coefficients of many liquid metals (at $T \approx 1{,}250$ °C) are in the range 100–4,000 μm^2/s [8, 18, 24] and the simulation results are practically independent of D_L in the mentioned range [8], an average value $D_L = 2{,}000$ μm^2/s is employed.
6. The initial thickness of the liquid, determined by the thickness of the amorphous ribbon, is about $a = 20$ μm.

The time needed to end the process as obtained from the simulation is about 230 min. This value is much greater than the time measured under a pressure of 4 MPa.

The fact that D is almost independent of pressure, indicates that the action of p is revealed on other variables, particularly the actual initial thickness. The actual initial thickness is less than the thickness of the amorphous ribbon, that is, due to the applied pressure the liquid Fe–B spills out of the gap between the steel tubes. Therefore, the actual initial thickness is unknown.

The initial thickness a is determined fitting the numerical expression of the duration of the process with the experimental value of the total time needed to complete the process.

The model data used are summarized in Table 2.

The effective initial thickness that fits the experimental value of the time needed to complete the TLPB process (7.0 min) is 2.9 μm. The time dependence of the liquid thickness $w(t)$, obtained from our numerical simulation, is shown in Fig. 5.

Table 2 Model parameters used for steel/iron–boron/steel joining

C_L (wt%)	C_S (wt%)	C_{XL} (wt%)	C_{XS} (wt%)
3.8	0	3.011	0.021
D_L (μm^2/s)	D_S (μm^2/s)	a (μm)	T(°C)
2,000	194	2.9	1,250

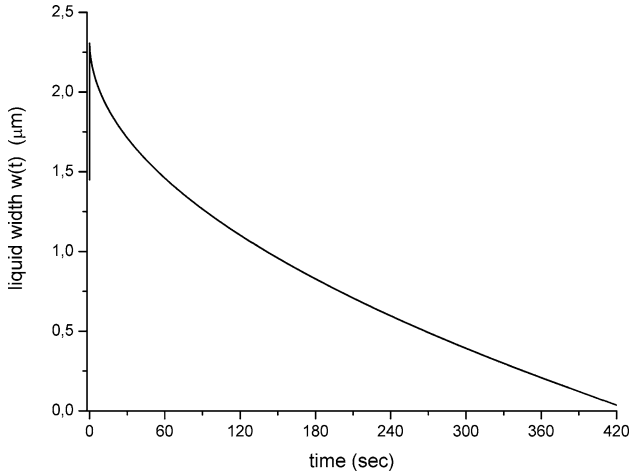

Fig. 5 Model results for steel/iron–boron/steel joining. The time dependence of the liquid width $w(t)$ is shown

Discussion

If the process is controlled by the surface tension alone, an elemental calculation of the initial thickness of the liquid gap can be carried out, concluding that the initial thickness is lower than 0.75 μm (The surface tension coefficient employed is $\gamma = 1.938$ J/m^2 corresponding to liquid iron at the melting temperature [25].). However, a real surface is never perfectly clean or perfectly smooth, and the area of metal-to-metal contact between surfaces can be a small fraction of the area of the pieces in contact. Though, as the joint zone is heated to high temperature, under compression, the initial roughness of the steel surfaces may result softened.

The use of the TLPB process allows the liquid phase to fill the voids in the joint obtaining an excellent contact between surfaces. The excess liquid, not retained by the surface tension or the rough surface, is expelled from the joint by the applied pressure. Hence, only a fraction of the initial liquid is utilized in the bonding process, decreasing the process time.

As a consequence $a = 2.9$ μm represents the initial thickness of the liquid gap assuming that the excess liquid spills out just at the initial moment. Nevertheless, this value is not necessarily a true initial value.

The expulsion of liquid is not instantaneous. In other words, liquid would spill out of the joint during the entire dissolution stage. At the same time the metal surface asperities may be flattened by pressure improving the metal to metal contact hence contributing to

the reduction of the actual initial thickness of the liquid gap. Therefore, the accuracy of a as the actual initial thickness depends on the complex dependence of the liquid thickness on viscosity and surface tension, both strongly dependent on temperature, and pressure.

In spite of the supposition of planar solid/liquid interface, the actual liquid gap thickness is not uniform. As a consequence, when the joining process has not finished completely, the joint line is not continuous, and zones with microstructural continuity alternate with dashes where the liquid phase has persisted until the end of the isothermal stage.

Conclusions

A model using finite element method has been developed. It simulates diffusion-controlled, two-phase, moving-interface problems.

The numerical model was then used to research TLPB of steel/iron–boron/steel. The total process time estimated from the actual initial conditions resulted several times greater than the experimental value. This difference is attributed to the effect of pressure that ejects liquid from the joining zone whereas softens the roughness of the metal surfaces. An effective initial thickness of the liquid gap of 2.9 μm was estimated (actual thickness of the interlayer was about 20 μm). As a consequence the isothermal stage time is reduced to 7 min.

Acknowledgements The authors acknowledge the ''Agencia Nacional de Promoción Científica y Tecnológica'' (ANPCyT) from Argentina and the company Siderca that along with the ''Universidad de Buenos Aires'', have supported this work through the PICTO 04603.

The unvaluable support of Dr. Peter Svenc who kindly provided the Fe–B glassy ribbon is also acknowledged.

References

1. Sinclair CW, Purdy GR, Morral JE (2000) Metall Mater Trans A 31A:1187
2. Ohsasa K, Shinmura T, Narita T (1999) J Phase Equilibria 20(3):199
3. Sinclair CW (1999) J Phase Equilibria 20(4):361
4. MacDonald WD, Eagar TW (1992) Annu Rev Mater Sci 22:23
5. Ikawa H, Nakao Y, Isai T (1979) Trans Jpn Weld Soc 10(1):25
6. Duvall DS, Owczarski WA, Paulonis DF (1974) Welding J 53:203
7. Tuah-Poku I, Dollar M, Massalski TB (1988) Metall Trans A 19A:675
8. Zhou Y, North TH (1993) Model Simul Mater Sci Eng 1:505
9. Illingworth TC, Golosnoy IO, Gergely V, Clyne TW (2005) J Mater Sci 40:1
10. Khan TI, Wallach ER (1995) J Mater Sci 30:5151
11. Kishi S, Maenosono T, Sato M (1999) U. S. Patent Number 5875954
12. Hamada M, Fukadal Y, Hueda M, Komizo Y (2000) U. S. Patent Number 6059175
13. Shimizu T, Horio H, Kito K, Inagaki S, Yamada R (2003) U. S. Patent Number 6592154 B2
14. Cain SR, Wilcox JR, Venkatraman R (1997) Acta Mater 45(2):701
15. Ikeuchi K, Zhou Y, Kokowa H, North TH (1992) Metall Trans A 23A:2905
16. Saida K, Zhou Y, North TH (1993) J Mater Sci 28:6427
17. Kaur I, Mishin Y, Gust W (1995) In: Fundamentals of grain and interphase boundary diffusion. John Wiley & Sons Ltd., New York, p 62
18. Philibert J, Rothman S (1991) In: Atom movements, diffusion and mass transport in solids. Les editions de physique, p 22, 563
19. Bathe KJ (1996) In: Finite elements procedure. Prentice Hall
20. ASM Handbook Volume 3, Alloy Phase Diagram
21. Mc Lellan RB, Ko C (1993) J Phys Chem Solids 54:465
22. Mehrer H (1996) Defect Diffusion Forum 129–130:57
23. Busby PE, Warga ME, Wells C (1953) Trans AIME, J Metals 197:1463
24. Bruson A, Gerl M (1979) Phys Rev B 19(12):6123
25. Schade J, McLean A, Miller WA (1986) In: Collings EW, Koch CC (eds) Undercooled alloy phases, proceedings of the 1986 Hume-Rothery memorial symposium, March 2–6, 1986. The Metallurgical Society, pp 233–248